

000 BEYOND NEURAL INCOMPATIBILITY: EASING CROSS- 001 SCALE KNOWLEDGE TRANSFER IN LARGE LANGUAGE 002 MODELS THROUGH LATENT SEMANTIC ALIGNMENT 003

004 **Anonymous authors**
 005

006 Paper under double-blind review
 007

008 ABSTRACT 009

010 Large Language Models (LLMs) encode vast amounts of knowledge in their mas-
 011 sive parameters, which is accessible to locate, trace, and analyze. Despite ad-
 012 vances in neural interpretability, it is still not clear how to transfer knowledge
 013 in a fine-grained manner, namely parametric knowledge transfer (PKT). A key
 014 problem is enabling effective and efficient knowledge transfer across LLMs of
 015 different scales, which is essential for achieving greater flexibility and broader
 016 applicability in transferring knowledge between LLMs. Due to neural incompat-
 017 ibility, referring to the architectural and parametric differences between LLMs of
 018 varying scales, existing methods that directly reuse layer parameters are severely
 019 limited. In this paper, we identify the semantic alignment in latent space as the
 020 fundamental prerequisite for LLM cross-scale knowledge transfer. Instead of di-
 021 rectly using the layer parameters, our approach takes activations as the medium
 022 of layer-wise knowledge transfer. Leveraging the semantics in latent space, our
 023 approach is simple and outperforms prior work, better aligning model behaviors
 024 across varying scales. Evaluations on four benchmarks demonstrate the efficacy of
 025 our method. Further analysis reveals the key factors easing cross-scale knowledge
 026 transfer and provides insights into the nature of latent semantic alignment.
 027

028 1 INTRODUCTION 029

030 Language is the channel that lets humans and today’s language models communicate, yet it throws
 031 away much of the fine detail that lives inside a model. When we teach a smaller model using
 032 instructions, explanations, or distilled datasets, we compress the teacher’s rich internal signals into
 033 text and lose structure that matters for behavior. A better way to transfer knowledge would move
 034 internal states directly, similar in spirit to the idea of brainwave communication where the sender
 035 shares what it is thinking rather than what it can say. Large language models make this idea practical
 036 because their parameters and hidden states are accessible. Prior work shows that we can analyze
 037 these internals, find where knowledge lives, and measure how specific parts influence predictions
 038 using attribution methods and information flow tools (Kokhlikyan et al., 2020; Yu & Ananiadou,
 039 2024; Ferrando & Voita, 2024; Chen et al., 2025). This sets up our motivation for better knowledge
 040 transfer, where a student should be able to receive those signals directly from a teacher without
 041 going through text. It promises less loss, lower cost, and more truthful transfer.
 042

043 We study this idea under parametric knowledge transfer. The goal is to move internal knowledge
 044 from a larger teacher to a smaller student so that the student acts more like the teacher. Prior work
 045 explores two routes in parameter space. Seeking extracts teacher parameters with sensitivity mea-
 046 sures, injects them into the student through a LoRA initialization, and then relies on post alignment
 047 fine tuning (Zhong et al., 2024). LaTen aligns parameter spaces before injection using a light map-
 048 ping to reduce the cost of later training (Tan et al., 2025). Both show that knowledge transfer is
 049 possible, but also report instability when the models differ in module design and parameter values,
 050 a gap described as *neural incompatibility* (Tan et al., 2025). In our analogy above, the “brainwave
 051 communication” corresponds to sharing layer outputs, not sharing layer parameters. We therefore
 052 treat activations as the medium of transfer and align semantics first, before any parameter updates.
 053

We propose SEMALIGN, a semantics-first method for parametric knowledge transfer that uses layer outputs as the transfer signal. SemAlign consists of three steps: First, we run layer attribution on the teacher to locate layers that carry task relevant signal and we pair them with compatible layers in the student. This follows evidence that neuron and concept relations are many to many and that robust layer selection matters (Yu & Ananiadou, 2024; Chen et al., 2025). Second, we align latent semantics for each paired layer. We decompose the teacher hidden states into semantic components in the teacher space and recombine them as supervisory hidden states in the student space. This treats aligned activations as supervision and follows results showing that shaping hidden states preserves meaning and supports stable adaptation (Gu et al., 2024; 2025; Kong et al., 2024). Third, we steer the student by optimizing the paired layers so that, on the same inputs, their outputs approach the aligned supervisory hidden states. In short, we align how layers behave rather than how weights look, which reduces neural incompatibility while keeping the procedure simple and efficient.

We evaluate SemAlign under the same setup as the prior work (Tan et al., 2025). We use four standard benchmarks on professional knowledge, mathematical reasoning and code generation. The experiments are conducted with Llama 2 models (Touvron et al., 2023), performing task related parametric knowledge transfer by pairing larger teachers with smaller students that differ in depth and width. Across all tasks, SemAlign improves student performance over task matched baselines and over parameter space transfer baselines. Two findings stand out: first, performing latent semantic alignment before any parameter update strongly predicts stable cross-scale transfer; second, steering a small set of paired layers is enough to induce broader behavioral alignment, which makes the method efficient in both compute and data. The replication repository is attached as supplementary material. To summarize, our contributions are as follows:

- We present a semantics-first view of parametric knowledge transfer for cross-scale language models. The formulation treats latent semantic alignment between paired layers as the prerequisite to transfer and uses layer outputs, not raw parameters, as the medium.
- We introduce SEMALIGN, which combines layer attribution and pairing, latent semantic alignment, and representation steering. This design addresses neural incompatibility that limits parameter space transfer in Seeking and LaTen (Zhong et al., 2024; Tan et al., 2025).
- We provide comprehensive experiments on extensive benchmarks with Llama 2. Results and analysis identify the key factors that ease cross-scale transfer and show consistent gains in the efficacy. We provide further discussion in the appendix.

2 RELATED WORK

2.1 KNOWLEDGE ATTRIBUTION IN LANGUAGE MODELS

Knowledge attribution studies methods for identifying where knowledge resides in large language models and how those components influence predictions. The focus has moved from layer level inspections to neuron level and path level analyses that scale to current models. One representative line designs a static, single pass neuron score that separates “query” and “value” neurons and avoids repeated gradient passes (Yu & Ananiadou, 2024). Moving from units to mechanisms, information flow routes rebuild prediction time computation as a sparse graph and show how influential parts work together during inference (Ferrando & Voita, 2024). In practical analyses, CAPTUM provides operators for layer and neuron attribution, including Internal Influence, Neuron Integrated Gradients, and DeepLIFT or SHAP, which many studies adopt as reproducible baselines (Kokhlikyan et al., 2020). Recent evidence also reports degenerate knowledge neurons, where different neuron sets encode the same fact; this observation supports concept aware or path aware selection when using attribution to guide editing or transfer (Chen et al., 2025).

2.2 SEMANTIC ANALYSIS AND LATENT SPACE ALIGNMENT

Semantic analysis and latent space alignment shape and match internal representations so that model adaptation preserves meaning rather than only optimizing an output loss. Within this view, a single research line proposes two connected methods that form a coherent pipeline. Vocabulary Defined Semantics (VDS) uses the model vocabulary to anchor directions in the hidden space and then clusters examples around these anchors, which stabilizes in context learning by better matching data to

108 the model’s internal semantic frame (Gu et al., 2024). Building on that foundation, Semantic Aware
 109 Layer Freezing (SALF) treats the structure exposed by VDS as semantic anchors at the layer level
 110 and freezes those parts while tuning the remainder, which preserves core semantics and works with
 111 parameter efficient finetuning and quantization (Gu et al., 2025). A complementary research thread
 112 adjusts hidden states at test time with small edits, showing that behavior can be steered through
 113 representation space without heavy retraining (Kong et al., 2024).

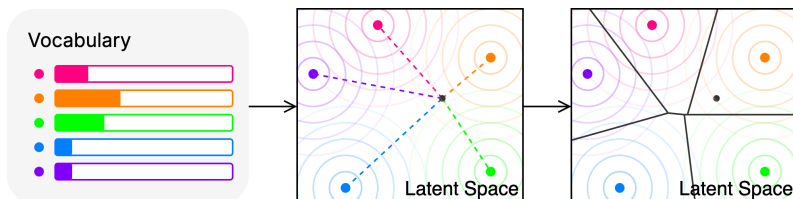
115 2.3 PARAMETRIC KNOWLEDGE TRANSFER

117 Knowledge transfer includes teacher and student distillation, representational matching across layers,
 118 and parameter mixing through model merging or task vectors. These approaches provide strong
 119 baselines and tools, yet they often work in the output space or assume closely related architectures
 120 (Xu et al., 2024; Yang et al., 2024; 2025; Liu et al., 2024). Recent studies frame the problem
 121 as parametric knowledge transfer, where the goal is to move internal knowledge that lives inside a
 122 model, including parameters and intermediate computations such as activations and residual streams.
 123 A representative system, SEEKING, extracts sensitive components from a source, injects them into
 124 a target through LoRA initialization, and then applies post alignment fine tuning; results indicate
 125 that cross-scale transfer is feasible and that alignment quality is important for stability (Zhong et al.,
 126 2024). Follow up work on Neural Incompatibility examines alignment as the main bottleneck cross
 127 scales and distinguishes two design choices: PostPKT, which follows extract, inject, and train, and
 128 PrePKT, exemplified by LaTen, which aligns parametric spaces with light training before transfer
 129 (Tan et al., 2025). Our method adopts semantics-first plan by using latent semantic alignment as
 130 a precondition for parametric knowledge transfer, to mitigate neural incompatibility.

131 3 MOTIVATIONAL ANALYSIS

132 3.1 PRELIMINARY: VOCABULARY-DEFINED SEMANTICS

135 For the recognizable semantic meanings of a given LM, *vocabulary-defined semantics* proposed
 136 defining a set of special representations in the latent space to associate with the labels on the vocabu-
 137 lary. It quantifies the semantic property of LM latent space leveraging local isotropy (Cai et al.,
 138 2021), and benefits parameter optimizations, such as efficient logits computation (Gu et al., 2024).
 139 For each label on the LM vocabulary, there is an associated representation in the latent space, termed
 140 as “semantic basis”, they share the same semantic meaning, as shown in Figure 1.



141
 142 Figure 1: Semantic association of vocabulary and latent space. For each color label on the vocabu-
 143 lary (left), there is a color semantic basis in the latent space (middle). The semantics of the dark dot
 144 (indicating an arbitrary representation) in the latent space can be quantified as its cosine similarities
 145 to semantic bases. The semantics can be computed as probabilities on the vocabulary. When focus-
 146 ing on the nearest semantic basis for a given latent representation, a latent space can be quantified
 147 as discrete semantic regions (right).

148 For a given LM-head matrix, we conduct matrix multiplication to obtain semantic bases in the latent
 149 space. Since the computation direction is from logits to representations, instead of using the LM-
 150 head matrix \mathbb{W} , we use its pseudoinverse \mathbb{W}^+ . If there are v labels in the vocabulary, there will be
 151 v unique semantic bases representing all semantic meanings. At the output side of LM, we multiply
 152 each onehot embedding \vec{e} by the pseudoinverse matrix \mathbb{W}^+ to obtain the corresponding representa-
 153 tion \vec{s} . That is, $\vec{s} = \vec{e} \cdot \mathbb{W}^+$. The computation is equivalent to solving the least squares problem of a
 154 system of linear equations. The time cost of computing semantic bases is rather low. For language
 155 models like LLaMA 2 (7B, 13B, and even 70B) which has 32000 labels in the vocabulary, it takes
 156 around 10 seconds on an A100 GPU. Moreover, this is a one-time computation with persistent value.

162
163

3.2 EMPIRICAL FINDING: VECTOR NATURE OF SEMANTICS

164
165
166
167
168
169
170
171
172

Centered on each semantic basis, there forms a “semantic field”. The concept of semantic field is similar to the *field* term in physics (such as electric field, then the semantic basis analogies to the electric pole). The semantics of an arbitrary latent representation can be quantified as the overlapping impact of numerous semantic fields, and be further computed as probabilities (Gu et al., 2024). The process is “composition of semantics”, where multiple *semantic components* become a *resultant vectors* via vector addition. Therefore, we propose a hypothesis that the overlapping effects of semantic fields support a corresponding reversed operation “resolution of semantics”. That is, a single *resultant vector* in latent space may be resolved into multiple *component vectors* along the directions of semantic bases.

173
174
175
176
177
178
179
180
181

In detail, for a given latent representation \vec{r} , its semantic meaning can be projected to different semantic bases to obtain corresponding semantic components $\vec{c}_i = \text{proj}(\vec{r}, \vec{s}_i)$ (analogy to “component force” in a force field). By accumulating the decomposed semantics, we get a “resultant semantics” $\sum_{i=1}^n \vec{c}_i$ (analogy to “resultant force” in a force field). The equation $\vec{r} \parallel \sum_{i=1}^n \vec{c}_i$ stands approximately true. In contrast, when taking a random collection of vectors as semantic bases and obtain $\vec{c}'_i = \text{proj}(\vec{r}, \vec{s}'_i)$, the equation $\vec{r} \perp \sum_{i=1}^n \vec{c}'_i$ stays true. It is consistent with the property of the latent space that, arbitrary vectors in a high-dimensional space tend to be orthogonal.

182
183
184
185
186
187
188
189
190
191

We conduct empirical experiments to validate the hypothesis. For a given data and LM, we first compute the outputs of each layer, and then decompose each layer outputs into semantic components and eventually recompose back as layer outputs. If the old layer outputs and the new layer outputs share almost similar direction in the latent space, namely their cosine similarity is high, the hypothesis stands. We run with Qwen3 model on HumanEval, to study whether the hypothesis stand with the output-side semantic bases, and using input-side semantic bases for comparison. As shown in Figure 2, the hypothesis stand with the case of using output-side semantic bases because of the very high cosine similarities no matter the layer. In contrast, the situation of using input-side semantic bases is bad and the cosine similarities is close to zero, which indicates the common phenomenon in high-dimensional latent space that arbitrary vectors tend to be orthogonal to each other.

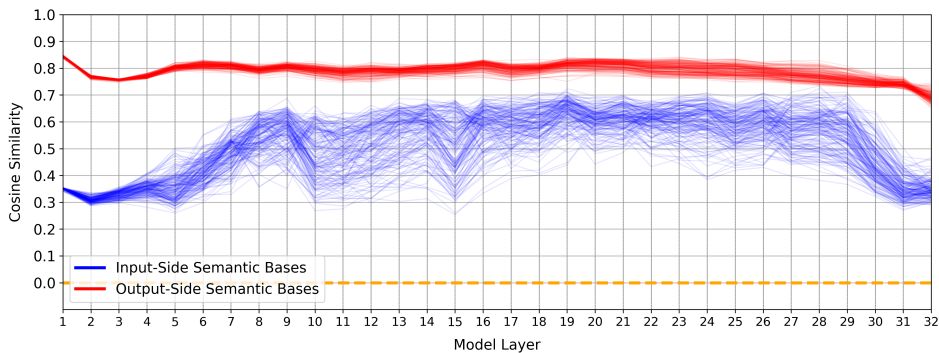
203
204
205

Figure 2: Empirical Validation of Semantics Decomposition on HumanEval with Llama2 (7B).

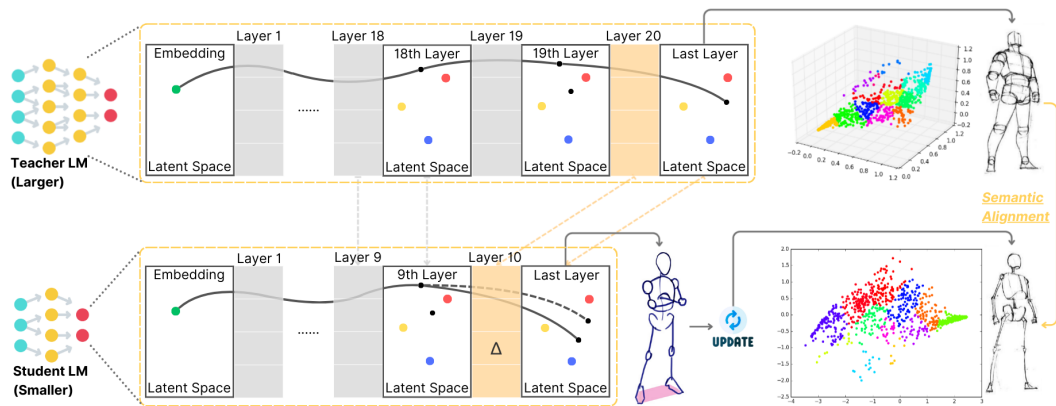
206
207

4 APPROACH

208
209
210
211
212
213
214
215

Our approach utilized LM semantics to align the latent space between certain layers of teacher and student models. The transferred knowledge by semantic alignment is layer outputs, as the supervisory signal for parameter optimization. We name our approach Semantic Alignment, short as SEMALIGN. The illustration of our approach is in Figure 3, and the main steps are: (1) First, we locate critical layers in teacher LM by attribution algorithm, and find the layer to pair in student LM by pairing strategy. The semantic alignment will happen between the pair layers, from teacher to student; (2) Then, we decompose the semantics of layer outputs in teacher’s latent space, and recompose as supervisory layer outputs in student’s latent space. It aligns latent spaces while preserving the semantics of layer outputs; (3) Further, in the student model, we optimize layer parameters using

216 the supervisory layer outputs. For the same given data, the layer outputs of the paired layers become
 217 close, indicating the similar behaviors by teacher and student models.
 218



219
 220
 221
 222
 223
 224
 225
 226
 227
 228
 229
 230
 231
 232
 233 Figure 3: Illustration of our cross-scale knowledge transfer approach. Assume a 20-layer teacher
 234 layers in teacher and student models are pairs by dashed arrow lines. Marked by orange color, the 20th teacher's layer is located as critical, and its pair is the
 235 10th student's layer, namely the layer to optimize. Second, represented by the dots in 3D and 2D spaces, the layer outputs from teacher model are decomposed in the larger dimensional teacher's
 236 latent space and recomposed in the smaller dimensional student's latent space, as the supervisory
 237 signal. It undergoes dimensional reduction but still preserves complete semantics, represented by the
 238 changes to gray dots, remaining the body gesture but reducing details. Third, the paired student's
 239 layer will be updated, to make the student's layer outputs be close to the supervisory signal. It is
 240 similar to blue dots, to be adjusted playing the same body gesture as gray dots does. After the cross-
 241 scale knowledge transfer, student's layer outputs will steer to the supervisory signal, represented by
 242 the dashed curve, and partial layer parameters are optimized, marked by the delta symbol. In the
 243 last layer's latent space, the model outputs are represented by the small dark dot whose distances to
 244 big color dots indicates the probabilities in LM vocabulary. For the teacher LM, its dark dot is close
 245 to the red dot, so its output label is the corresponding red label; while for the student LM, its output
 246 label was the corresponding blue but will become red after knowledge transfer, since its dark dot
 247 moves far away from the blue dot while approaching the red dot.
 248

249 250 4.1 LAYER ATTRIBUTION AND LAYER PAIRING 251

252 **Layer Attribution.** We identify candidate teacher layers using *Layer Gradient* \times *Activation* at
 253 the layer level: for each layer, we multiply the gradient of the supervised objective by the layer's
 254 activations and aggregate over tokens and channels to obtain a scalar importance score per layer.
 255 This choice is simple, stable, and available in standard attribution toolkits (Kokhlikyan et al., 2020).

256 **Layer Pairing.** Let the teacher have L_T layers and the student have L_S layers. We build a depth-
 257 aware mapping that assigns each student layer a teacher counterpart while preserving order. For
 258 student index $k \in \{1, \dots, L_S\}$, define
 259

$$\ell_k^T = \max\left(1, \left\lfloor \frac{L_T}{L_S} k \right\rfloor\right) \in \{1, \dots, L_T\},$$

260 which, for example, gives $\ell_k^T = 2k$ when $L_T=20$ and $L_S=10$. This mapping is one-to-one when
 261 L_T/L_S is an integer; otherwise, some teacher layers may be shared across adjacent student layers.
 262 If a teacher layer ℓ_\star^T is judged critical by attribution but does not coincide with any ℓ_k^T , we select the
 263 nearest *deeper-or-equal* student index
 264

$$k^\dagger = \min \{ k' \in \{1, \dots, L_S\} : \ell_{k'}^T \geq \ell_\star^T \},$$

265 defaulting to $k^\dagger=L_S$ if the set is empty. We then operate on the pair $(\ell_{k^\dagger}^T, k^\dagger)$, which preserves
 266 depth order and guarantees a concrete student partner for every attributed teacher layer.
 267

If supervision requires a target at an exact student depth while L_T/L_S is non-integer, we interpolate between adjacent teacher layers. Let the student depth be k^\dagger and set $\rho = k^\dagger/L_S$. Define $u = L_T\rho$, then

$$a = \max(1, \min(|u|, L_T-1)), \quad b = a+1, \quad \lambda = \text{clip}(u - a, 0, 1).$$

Given teacher representations $\mathbf{h}_{(a)}^T$ and $\mathbf{h}_{(b)}^T$ at the supervision interface, the interpolated target for student layer k^\dagger is

$$\tilde{\mathbf{h}}^T = (1 - \lambda) \mathbf{h}_{(a)}^T + \lambda \mathbf{h}_{(b)}^T.$$

This yields a well-defined supervisory signal from the teacher for every student depth while respecting layer ordering.

4.2 LATENT SEMANTIC ALIGNMENT (TEACHER → STUDENT)

We construct a training-free, semantics-preserving mapping from a *teacher* layer’s latent space to a *student* layer’s latent space. The teacher and student come from the same LM family at different scales, and their semantic bases are index-aligned (Section Preliminaries). The idea is to *decompose* the teacher vector into components along teacher semantic atoms and *recompose* those components in the student basis using the *same* coefficients.

Let $\mathbf{h}^T \in \mathbb{R}^{D_T}$ be a teacher-layer output at the supervision interface and $\mathbf{h}^S \in \mathbb{R}^{D_S}$ a student-layer vector (to be constructed as a target). Let $S_T = [\mathbf{s}_1^T, \dots, \mathbf{s}_m^T] \in \mathbb{R}^{D_T \times m}$ and $S_S = [\mathbf{s}_1^S, \dots, \mathbf{s}_m^S] \in \mathbb{R}^{D_S \times m}$ denote the teacher and student semantic bases, respectively, with column i in S_T and S_S referring to the same semantic atom. Assume unit-normalized columns: $\|\mathbf{s}_i^T\|_2 = \|\mathbf{s}_i^S\|_2 = 1$.

Semantics-preserving Decomposition and Recomposition. We form *semantic coefficients* by cosine projection in the teacher space:

$$\mathbf{a} = [\cos(\mathbf{h}^T, \mathbf{s}_1^T), \dots, \cos(\mathbf{h}^T, \mathbf{s}_m^T)]^\top = \frac{S_T^\top \mathbf{h}^T}{\|\mathbf{h}^T\|_2} \in \mathbb{R}^m. \quad (1)$$

We then *recompose* in the student space with the same coefficients:

$$\tilde{\mathbf{h}}^S = S_S \mathbf{a} \in \mathbb{R}^{D_S}. \quad (2)$$

The vector $\tilde{\mathbf{h}}^S$ serves as the supervisory signal for the student layer output at the same interface.

Because column i of S_T and S_S denote the same semantic atom and all columns are unit-norm, the pair (decompose in teacher: $\mathbf{a} = S_T^\top \mathbf{h}^T / \|\mathbf{h}^T\|_2$, recompose in student: $\tilde{\mathbf{h}}^S = S_S \mathbf{a}$) transfers an identical set of component weights from teacher to student. Thus, the semantic content is preserved; only the ambient basis changes (teacher vs. student).

4.3 COSINE-ONLY LAYER AND OUTPUT ALIGNMENT

We adapt the student by updating only the parameters of its paired layer k while freezing all others. The training objective consists of *two* cosine-alignment terms with no additional weights: (i) a *layer-level* cosine loss that aligns the k -th layer’s activations to the semantics-preserving target, and (ii) an *output-level* cosine loss that aligns the final-layer logits to the supervised label direction. This naming emphasizes that both the intermediate representation (for semantic alignment) and the model output (a geometric surrogate of cross-entropy) are optimized using cosine similarity alone.

Let $\theta^{(k)}$ denote the parameters of student layer k . Let $\mathbf{h}^{(k)} \in \mathbb{R}^{B \times T \times D}$ be the student activations at a fixed supervision interface, chosen as the sublayer output *before* residual addition. Let $\mathbf{h}_*^{(k)} \in \mathbb{R}^{B \times T \times D}$ be the semantics-preserving target instantiated at the same interface (broadcast across batch/tokens as appropriate). Let $\mathbf{z} \in \mathbb{R}^{B \times T \times |\mathcal{Y}|}$ be the final-layer logits, and let $\mathbf{y}^{oh} \in \{0, 1\}^{B \times T \times |\mathcal{Y}|}$ be one-hot (or label-smoothed) target distributions over \mathcal{Y} .¹

The total training objective is an unweighted sum of these two terms: $\mathcal{L}(\theta^{(k)}) = \mathcal{L}_{\text{layer}} + \mathcal{L}_{\text{out}}$. The first term $\mathcal{L}_{\text{layer}} = 1 - \text{Avg}[\cos(\mathbf{h}^{(k)}, \mathbf{h}_*^{(k)})]$ represents the targeted layer’s alignment (semantic alignment at layer k); while the second term $\mathcal{L}_{\text{out}} = 1 - \text{Avg}[\cos(\mathbf{z}, \mathbf{y}^{oh})]$ represents the last

¹For instance-level tasks, use per-example logits $\mathbf{z} \in \mathbb{R}^{B \times |\mathcal{Y}|}$ and one-hot targets $\mathbf{y}^{oh} \in \{0, 1\}^{B \times |\mathcal{Y}|}$.

layer’s alignment (geometric surrogate of CE at the last layer). Besides, $\text{Avg}[\cdot]$ denotes a simple average over supervised positions, and $\cos(\mathbf{u}, \mathbf{v}) = \frac{\langle \mathbf{u}, \mathbf{v} \rangle}{\|\mathbf{u}\|_2 \|\mathbf{v}\|_2}$.

The first term, $\mathcal{L}_{\text{layer}}$, enforces *latent semantic alignment*: it drives the k -th layer’s representation toward the semantics-preserving target constructed by decomposing the teacher’s output into teacher semantic components and recomposing them in the student basis. The second term, \mathcal{L}_{out} , aligns the final logits with the ground-truth direction in label space; because cosine similarity is scale-invariant in the logit space, this term acts as a principled geometric surrogate for cross-entropy, encouraging the model to place probability mass on the correct label while avoiding sensitivity to logit scale. Together, the two cosine objectives couple representation-level semantics with output-level correctness using a single, consistent geometric criterion.

We backpropagate through the full network but update only $\theta^{(k)}$. The target $\mathbf{h}_*^{(k)}$ and the label vectors \mathbf{y}^{oh} are treated as constants. Matching the supervision interface for $\mathbf{h}^{(k)}$ and $\mathbf{h}_*^{(k)}$ (both pre-residual) ensures that the alignment term acts directly on the representation controlled by layer k , while the output cosine term refines the model’s decision geometry at the final layer.

5 EXPERIMENTS

In the experiments, we mainly study how our approach performs in parametric knowledge transfer comparing with PKT baselines. We also conduct analysis based on the latent representation similarities between teacher and student’s models before and after latent semantic alignment.

5.1 SETUP

Datasets. We use four well-established benchmarks, covering the most common downstream tasks: MMLU measures professional knowledge (Hendrycks et al., 2021); GSM8K measures mathematical reasoning (Cobbe et al., 2021); HumanEval and MBPP measure code generation (Chen et al., 2021; Austin et al., 2021).

Models. We conduct experiments with Llama 2 (Touvron et al., 2023) models, mainly chat versions instead of base versions for the better instruction-following ability. Besides, we employ LM variants to study the transfer from further-finetuned teacher models to a same student model, CodeLlama-13B-Python (Roziere et al., 2023) and WizardCoder-13B-Python (Luo et al., 2023). They are finetuned on Llama-2-13B with massive code data for an enhanced coding performance.

Metrics. For MMLU and GSM8K, we calculate *accuracy* in zero-shot setting; and for HumanEval and MBPP, we calculate *pass@1*. Larger scores mean better performance.

Baselines. The prior work on parametric knowledge transfer is SEEKING and LATEN, which are the baselines in our experiments. Both perform parametric knowledge transfer in two stages: Seeking is PostPKT (inject-then-train) while LaTen is PrePKT (align-then-inject). SEEKING first *extracts* task-relevant parameters from a teacher by ranking weights via sensitivity scores (gradient \times parameter on a seed set), then *injects* them into a student. Layer-wise importance is aggregated to pick the top layers; within each selected matrix, a high-sensitivity sub-block is chosen to bridge width/depth gaps. Each extracted block is SVD-factorized to initialize a low-rank LoRA (B, A), after which the student is post-aligned by standard fine-tuning. LATEN adopts a *Locate-Then-Align* pipeline to minimize post-training. It *locates* neuron-level carriers of knowledge in FFN/MHSA using static attribution, selects top neurons per layer, and forms teacher-side deltas. A lightweight hypernetwork g_ϕ is trained on a tiny alignment set to *pre-align* these deltas into the student’s parameter shape/scale, which are then injected once for immediate gains. This design targets cross-model incompatibilities by aligning deltas before injection rather than SVD-to-LoRA initialization plus post-alignment.

5.2 RESULTS

Results of Cross-Scale Knowledge Transfer. In all four benchmarks, SEMALIGN improves substantially over Llama2-7B-Chat while remaining below the Llama2-13B-Chat teacher, and it stays closer to the teacher than the other transfer baselines on average. Concretely, the absolute gaps

378 between SemAlign and 13B are 2.60 (MMLU: 50.30 vs 52.90), 1.34 (GSM8K: 19.21 vs 20.55),
 379 1.41 (HumanEval: 17.34 vs 18.75), and 0.42 (MBPP: 18.78 vs 19.20), averaging 1.44 points. This
 380 average gap is smaller than SEEKING (\approx 3.92) and LATEN (\approx 3.43). A per-task view shows
 381 one exception—on GSM8K, LaTen (20.47) is numerically closest to 13B (20.55)—while SEEKING
 382 overshoots the teacher (28.23). Overall, SemAlign’s three-of-four closer margins indicate it learns
 383 the teacher’s behavior more faithfully than the baselines.

Models	MMLU	GSM8K	HumanEval	MBPP
Llama2-7B-Chat	44.20	16.07	14.05	17.80
Llama2-13B-Chat	52.90	20.55	18.75	19.20
Seeking	49.60	28.23	15.44	20.60
LaTen	44.40	20.47	14.63	18.20
SemAlign	50.30	19.21	17.34	18.78

392 Table 1: Results of Parametric Knowledge Transfer in Diverse Downstream Tasks.
 393
 394

395 On task leadership, SemAlign attains the best transferred performance on MMLU (50.30) and
 396 HumanEval (17.34), surpassing both Seeking (49.60, 15.44) and LATEN (44.40, 14.63), whereas
 397 SEEKING leads on GSM8K (28.23) and MBPP (20.60). Notably, SEEKING exceeds the 13B teacher
 398 on both GSM8K (+7.68) and MBPP (+1.40), while SemAlign remains below but close to the
 399 teacher; this pattern is consistent with SemAlign’s cosine-similarity objective encouraging conser-
 400 vative matching of teacher representations, whereas SEEKING appears to incorporate additional pa-
 401 rameter optimization beyond pure transfer.

402 An additional observation is the stability–aggressiveness trade-off across methods: SEEKING
 403 achieves large gains on reasoning- and coding-flavored datasets by overshooting the teacher
 404 (GSM8K, MBPP), suggesting stronger task-specific optimization, while SemAlign stays within
 405 ≤ 2.60 points of the teacher on every task, indicating steadier transfer that narrows the gap without
 406 over-amplifying particular skills.

407 **Results of Knowledge Transfer from Finetuned Models.** SEMALIGN consistently outperforms
 408 the transfer baselines in five of six teacher–task settings, indicating stronger parametric knowledge
 409 transfer. With Llama2-13B-Chat as teacher, it leads LATEN and SEEKING on HumanEval (17.34
 410 vs 14.63/15.44), and only trails SEEKING on MBPP (18.78 vs 20.60). The advantage becomes
 411 clearer with code-specialized teachers: from CodeLlama-13B-Python, SemAlign reaches 20.12
 412 (+4.07 over SEEKING, +6.10 over LATEN) on HumanEval and 22.35 (+0.95, +4.55) on MBPP;
 413 from WizardCoder-13B-Python, it attains 19.46 (+4.42, +5.44) and 21.18 (+1.38, +2.58) on Hu-
 414 manEval and MBPP, respectively. These trends show that SemAlign extracts and transfers teacher
 415 competency more reliably, especially when the teacher is stronger in coding.

Models	HumanEval	MBPP
Llama2-7B-Chat	14.05	17.80
Llama2-13B-Chat	18.75	19.20
Seeking	15.44	20.60
LaTen	14.63	18.20
SemAlign	17.34	18.78
CodeLlama-13B-Python	47.56	37.80
Seeking	16.05	21.40
LaTen	14.02	17.80
SemAlign	20.12	22.35
WizardCoder-13B-Python	56.71	41.60
Seeking	15.04	19.80
LaTen	14.02	18.60
SemAlign	19.46	21.18

431 Table 2: Results of Parametric Knowledge Transfer from Finetuned Teacher Models.

432 Across two coding benchmarks, all methods remain far below the finetuned teachers (CodeLlama-
 433 13B-Python: 47.56/37.80; WizardCoder-13B-Python: 56.71/41.60), despite often surpassing
 434 Llama2-7B-Chat and sometimes even matching or exceeding Llama2-13B-Chat (e.g., SEEKING on
 435 MBPP with 20.60 vs 19.20). This gap suggests that the extensive, task-specific optimization baked
 436 into code-specialized teachers is difficult to reconstruct via short-horizon transfer; objectives like
 437 cosine matching encourage conservative alignment to teacher representations rather than aggressive
 438 task re-optimization, limiting the attainable ceiling without longer or more targeted finetuning.

439 An additional observation is that SEEKING only overshoots the teacher on MBPP when the teacher
 440 is the generalist Llama2-13B-Chat (20.60 > 19.20) but not when the teacher is code-specialized;
 441 meanwhile, SEMALIGN shows its largest margins over baselines precisely when transferring from
 442 code-specialized teachers. This pattern hints that aggressive, task-specific optimization in SEEK-
 443 ING can exploit headroom left by generalist teachers, whereas SemAlign’s representation-faithful
 444 transfer scales better with teacher specialization.

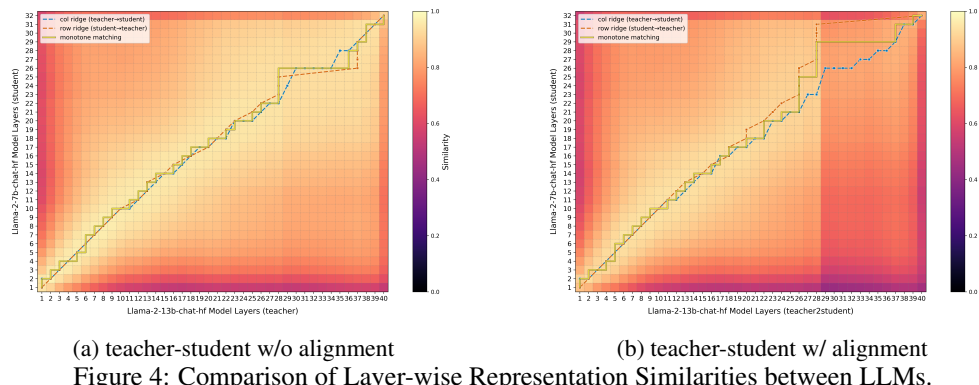
445

446 5.3 ANALYSIS

447

448 We adopt Centered Kernel Alignment (CKA) (Kornblith et al., 2019) as the analysis tool to study
 449 the similarities between layer outputs from teacher and student models. We run Llama2-chat models
 450 on HumanEval data. CKA is commonly used to compute the similarities between feature repres-
 451 entations in neural networks, which is based on Hilbert-Schmidt Independence Criterion (HSIC).

452 As shown in Figure 4, there are high similarities between the layer outputs from teacher and student
 453 models, especially along the main diagonal. It indicates that, there exists no neuron incompatibility if
 454 using layer outputs as the medium of parametric knowledge transfer, instead of directly using layer
 455 parameters. The highest similarities is almostly layer-by-layer, from shallow to deep. Meanwhile,
 456 the cases before (the left subfigure) and after (the right subfigure) latent semantic alignment share
 457 very similar pattern of similarities. It means, adopting latent space alignment is a safe way to utilize
 458 the similarities between layer outputs between cross-scale language models.



(a) teacher-student w/o alignment

(b) teacher-student w/ alignment

Figure 4: Comparison of Layer-wise Representation Similarities between LLMs.

470

471

472

473 6 CONCLUSION

474

475

476

477

478

479

480

481

482

483

484

485

We studied parametric knowledge transfer across differently scaled LLMs from a *semantics-first* perspective. Rather than moving raw parameters as in prior paradigms, we use layer outputs as the medium of transfer and identify *latent semantic alignment* as the prerequisite for stable cross-scale transfer. Building on this view, SEMALIGN locates and pairs teacher and student layers, aligns their latent semantics, and then steers the student so its paired layers reproduce the aligned supervisory hidden states. This design avoids neural incompatibility, simplifies the procedure, and makes transfer efficient in both compute and data. Empirically, SemAlign improves students over task-matched baselines and over parameter-space transfer methods on four benchmarks with Llama 2 families. The results support our central claim: treating activations as the carrier of knowledge and aligning semantics-first provides a robust path to cross-scale PKT.

486 REFERENCES
487

488 Zeyuan Allen-Zhu and Yuanzhi Li. Physics of language models: Part 3.3, knowledge capacity
489 scaling laws. In *The Thirteenth International Conference on Learning Representations*.

490 Jacob Austin, Augustus Odena, Maxwell Nye, Maarten Bosma, Henryk Michalewski, David Dohan,
491 Ellen Jiang, Carrie Cai, Michael Terry, Quoc Le, et al. Program synthesis with large language
492 models. *arXiv preprint arXiv:2108.07732*, 2021.

493

494 Xingyu Cai, Jiaji Huang, Yu-Lan Bian, and Kenneth Ward Church. Isotropy in the contextual embed-
495 ding space: Clusters and manifolds. In *International Conference on Learning Representations*,
496 2021. URL <https://api.semanticscholar.org/CorpusID:235614342>.

497

498 Mark Chen, Jerry Tworek, Heewoo Jun, Qiming Yuan, Henrique Ponde De Oliveira Pinto, Jared
499 Kaplan, Harri Edwards, Yuri Burda, Nicholas Joseph, Greg Brockman, et al. Evaluating large
500 language models trained on code. *arXiv preprint arXiv:2107.03374*, 2021.

501

502 Yuheng Chen, Pengfei Cao, Yubo Chen, Yining Wang, Shengping Liu, Kang Liu, and Jun Zhao.
503 Cracking factual knowledge: A comprehensive analysis of degenerate knowledge neurons in large
504 language models. In *Proceedings of ACL 2025*, 2025. URL <https://aclanthology.org/2025.acl-long.505/>.

505

506 Karl Cobbe, Vineet Kosaraju, Mohammad Bavarian, Mark Chen, Heewoo Jun, Lukasz Kaiser,
507 Matthias Plappert, Jerry Tworek, Jacob Hilton, Reiichiro Nakano, et al. Training verifiers to
508 solve math word problems. *arXiv preprint arXiv:2110.14168*, 2021.

509

510 Javier Ferrando and Elena Voita. Information flow routes: Automatically interpreting language
511 models at scale. In *Proceedings of EMNLP 2024*, 2024. doi: 10.18653/v1/2024.emnlp-main.965.
512 URL <https://aclanthology.org/2024.emnlp-main.965/>.

513

514 Jian Gu, Aldeida Aleti, Chunyang Chen, and Hongyu Zhang. Vocabulary-defined semantics: Latent
515 space clustering for improving in-context learning. *arXiv preprint arXiv:2401.16184*, 2024. URL
<https://arxiv.org/abs/2401.16184>.

516

517 Jian Gu, Aldeida Aleti, Chunyang Chen, and Hongyu Zhang. A semantic-aware layer-freezing
518 approach to computation-efficient fine-tuning of language models. In *Findings of the Association
519 for Computational Linguistics: ACL 2025*, 2025. doi: 10.18653/v1/2025.findings-acl.420. URL
<https://aclanthology.org/2025.findings-acl.420/>.

520

521 Dan Hendrycks, Collin Burns, Saurav Kadavath, Akul Arora, Steven Basart, Eric Tang, Dawn Song,
522 and Jacob Steinhardt. Measuring mathematical problem solving with the math dataset. *arXiv
523 preprint arXiv:2103.03874*, 2021.

524

525 Narine Kokhlikyan, Vivek Miglani, Miguel Martin, Edward Wang, Bilal Alsallakh, Jonathan
526 Reynolds, Alexander Melnikov, Natalia Kliushkina, Carlos Araya, Siqi Yan, and Orion Reblitz-
527 Richardson. Captum: A unified and generic model interpretability library for pytorch, 2020. URL
<https://arxiv.org/abs/2009.07896>.

528

529 Lingkai Kong et al. Aligning large language models with representation editing. In *Ad-
530 vances in Neural Information Processing Systems 37 (NeurIPS 2024)*, 2024. URL
531 https://proceedings.neurips.cc/paper_files/paper/2024/file/41bba7b0f5c81e789a20bb16a370aeeb-Paper-Conference.pdf.

533

534 Simon Kornblith, Mohammad Norouzi, Honglak Lee, and Geoffrey Hinton. Similarity of neural
535 network representations revisited. In *International conference on machine learning*, pp. 3519–
536 3529. PMIR, 2019.

537

538 Woosuk Kwon, Zhuohan Li, Siyuan Zhuang, Ying Sheng, Lianmin Zheng, Cody Hao Yu, Joseph E.
539 Gonzalez, Hao Zhang, and Ion Stoica. Efficient memory management for large language model
serving with pagedattention. In *Proceedings of the ACM SIGOPS 29th Symposium on Operating
Systems Principles*, 2023.

540 Ziyue Liu et al. Model merging in llms, mllms, and beyond: Methods, theories, applications, and
 541 opportunities. *arXiv preprint arXiv:2408.07666*, 2024. URL <https://arxiv.org/abs/2408.07666>.

543

544 Ziyang Luo, Can Xu, Pu Zhao, Qingfeng Sun, Xiubo Geng, Wenxiang Hu, Chongyang Tao, Jing
 545 Ma, Qingwei Lin, and Dixin Jiang. Wizardcoder: Empowering code large language models with
 546 evol-instruct. *arXiv preprint arXiv:2306.08568*, 2023.

547

548 Adam Paszke, Sam Gross, Francisco Massa, Adam Lerer, James Bradbury, Gregory Chanan, Trevor
 549 Killeen, Zeming Lin, Natalia Gimelshein, Luca Antiga, Alban Desmaison, Andreas Köpf, Edward
 550 Yang, Zach DeVito, Martin Raison, Alykhan Tejani, Sasank Chilamkurthy, Benoit Steiner,
 551 Lu Fang, Junjie Bai, and Soumith Chintala. Pytorch: An imperative style, high-performance deep
 552 learning library. In *Neural Information Processing Systems*, 2019.

553

554 Baptiste Roziere, Jonas Gehring, Fabian Gloeckle, Sten Sootla, Itai Gat, Xiaoqing Ellen Tan, Yossi
 555 Adi, Jingyu Liu, Romain Sauvestre, Tal Remez, et al. Code llama: Open foundation models for
 556 code. *arXiv preprint arXiv:2308.12950*, 2023.

557

558 Yuqiao Tan, Shizhu He, Kang Liu, and Jun Zhao. Neural incompatibility: The unbridgeable gap of
 559 cross-scale parametric knowledge transfer in large language models. In *Proceedings of the 63rd Annual
 560 Meeting of the Association for Computational Linguistics (Long Papers)*, pp. 21586–21601, 2025. doi: 10.18653/v1/2025.acl-long.1047. URL <https://aclanthology.org/2025.acl-long.1047/>.

561

562 Hugo Touvron, Thibaut Lavril, Gautier Izacard, Xavier Martinet, Marie-Anne Lachaux, Timothée
 563 Lacroix, Baptiste Rozière, Naman Goyal, Eric Hambro, Faisal Azhar, et al. Llama: Open and
 564 efficient foundation language models. *arXiv preprint arXiv:2302.13971*, 2023.

565

566 Thomas Wolf, Lysandre Debut, Victor Sanh, Julien Chaumond, Clement Delangue, Anthony Moi,
 567 Pierrick Cistac, Tim Rault, Rémi Louf, Morgan Funtowicz, and Jamie Brew. Transformers: State-
 568 of-the-art natural language processing. In *Conference on Empirical Methods in Natural Language
 569 Processing*, 2019.

570

571 Xiaohan Xu, Ming Li, Chongyang Tao, Tao Shen, Reynold Cheng, Jinyang Li, Can Xu, Dacheng
 572 Tao, and Tianyi Zhou. A survey on knowledge distillation of large language models. *arXiv
 573 preprint arXiv:2402.13116*, 2024. URL <https://arxiv.org/abs/2402.13116>.

574

575 Chuanpeng Yang, Wang Lu, Yao Zhu, Yidong Wang, Qian Chen, Chenlong Gao, Bingjie Yan, and
 576 Yiqiang Chen. Survey on knowledge distillation for large language models: Methods, evaluation,
 577 and application. *arXiv preprint arXiv:2407.01885*, 2024. URL <https://arxiv.org/abs/2407.01885>.

578

579 Enneng Yang et al. A review of model merging approaches. *arXiv preprint arXiv:2503.08998*, 2025.
 580 URL <https://arxiv.org/abs/2503.08998>.

581

582 Zeping Yu and Sophia Ananiadou. Neuron-level knowledge attribution in large language models.
 583 In *Proceedings of the 2024 Conference on Empirical Methods in Natural Language Processing*,
 2024. URL <https://aclanthology.org/2024.emnlp-main.191/>.

584

585 Ming Zhong, Chenxin An, Weizhu Chen, Jiawei Han, and Pengcheng He. Seeking neural nuggets:
 586 Knowledge transfer in large language models from a parametric perspective. In *Proceedings
 587 of the International Conference on Learning Representations (ICLR)*, 2024. URL <https://openreview.net/forum?id=mIEHICHG0o>.

588

589

590 **A IMPLEMENTATION DETAILS**

591

592 **A.1 STATS OF LANGUAGE MODELS**

593

The stats of language models in our experiments are shown in Table 3.

	Llama2		CodeLlama	WizardCoder
	7B	13B	13B	13B
Head Num.	32	40	40	40
Layer Num.	32	40	40	40
Dimension	4,096	5,120	5,120	5,120
Vocabulary	32,000	32,000	32,000	32,001

Table 3: Stats of Llama 2 Language Models.

A.2 IMPLEMENTATIONS DETAILS

We follow the experimental protocol of LATEN for a fair comparison, but unlike LaTen, our approach uses a single training phase only: the alignment operation is integrated into the training objective as an auxiliary loss term, with no separate alignment stage or post-training optimization. In detail, we fine-tune the smaller model for 5 epochs with a batch size of 64 and a learning rate of 3×10^{-4} (for HUMAN EVAL, 3×10^{-5}), and use 3 epochs in the SFT setting; LoRA uses rank $r=16$ and is inserted into FFN (up_proj, down_proj) and MHSA (v_proj, o_proj) modules. For baseline reproduction under LATEN’s protocol, the hypernetwork is trained with a learning rate of 1×10^{-5} and weight decay 0.05, the sample size is $P=16$, and 10% of neurons are transferred per layer. The hyperparameters on alignment and trainment are shown in Table 4 and Table 5.

Our implementation uses deep learning framework PYTORCH (Paszke et al., 2019), TRANSFORMERS (Wolf et al., 2019) and vLLM (Kwon et al., 2023).

	MMLU	GSM8K	HumanEval	MBPP
Steps	2	4	3	8
Align Size	32	64	48	128
Learning Rate	3e-5	3e-5	3e-5	3e-5

Table 4: Implementation Details in Alignment.

	MMLU	GSM8K	HumanEval	MBPP
Epochs	5	5	3	5
Train Size	1000	1000	1000	300
Learning Rate	3e-4	3e-4	3e-5	3e-4

Table 5: Implementation Details in Training.

B DETAILS OF PARAMETRIC KNOWLEDGE TRANSFER BASELINES

Both baselines view knowledge as model weights and use the same two-step process: *extract* from the teacher, then *inject* into the student. They also handle layer/width mismatches and are tested on multiple LLM benchmarks. SEEKING focuses on sensitivity-based selection and LoRA initialization, followed by post-training alignment, so its alignment cost comes after injection but yields stable gains. LATEN focuses on neuron-level localization and hypernetwork pre-alignment, shifting the cost upfront to reduce or avoid post-training; in doing so, it highlights neural incompatibility and motivates semantics-first alignment. The detailed technical descriptions are as follows:

B.1 ILLUSTRATE SEEKING

SEEKING treats parametric knowledge transfer as two stages: *extract* task-related parameters from a larger teacher, then *inject* them into a smaller student and perform *post-alignment* fine-tuning. Given a task \mathcal{T} and a small *seed* set produced by the teacher (typically a few dozen decoded examples),

SEEKING assigns an importance score to each teacher parameter θ_i via *sensitivity*:

$$S_{i,j}^T = \left| \theta_i^\top \nabla_{\theta_i} \mathcal{L}(x_j^T, y_j^T | \Theta) \right|, \quad S_i^T = \sum_{j=1}^k S_{i,j}^T,$$

a first-order approximation of the loss increase if θ_i were removed. Layer scores are obtained by summing parameter sensitivities within the layer; the top L_s layers (order-preserving) are kept for transfer. To bridge depth/width mismatches, SEEKING performs *sensitivity-guided dimensionality reduction* on each selected weight matrix $W^l \in \mathbb{R}^{n_l \times m_l}$ by choosing a submatrix $W_{\text{extract}}^l \in \mathbb{R}^{n_s \times m_s}$ (rows/columns or 2D block) that maximizes cumulative sensitivity:

$$W_{\text{extract}}^l = \arg \max_{W' \subseteq W^l} \sum_{\theta_i \in W'} S_i \quad \text{s.t. } n_s \leq n_l, m_s \leq m_l.$$

The extracted blocks across layers are aggregated into $\Delta\Theta_{\text{extract}}$. For *injection*, each W_{extract}^l is factorized with SVD, $U\Sigma V^\top$, to initialize a rank- r LoRA pair (B, A) via $B \leftarrow U_{[:,1:r]} \Sigma_{1:r,1:r}$ and $A \leftarrow V_{1:r,:}^\top$, yielding an initialized student

$$W^{l*} = W^l - W_{\text{extract}}^l + BA,$$

after which the student is fine-tuned to align the injected deltas. Empirically, SEEKING reports consistent gains across reasoning, professional knowledge, instruction-following, and open-domain dialogue, and analyzes factors such as teacher scale, initialization strategy, seed count, module origin, and LoRA rank.

B.2 ILLUSTRATE LATEN

LATEN formalizes two PKT regimes: *PostPKT* (inject then train-to-align) and *PrePKT* (align then inject). It proposes *Locate-Then-Align* to reduce or avoid post-training. For a larger teacher M_ℓ with parameters Θ_ℓ and a smaller student M_s with Θ_s , LaTen first *locates* the most informative sites at *neuron* granularity, then learns a light *hypernetwork* to *pre-align* teacher deltas to the student's parameter space before injection:

$$\Delta\Theta_\ell \leftarrow \text{Locate}(M_\ell; \mathcal{D}_{\text{extract}}), \quad \widehat{\Delta\Theta}_s \leftarrow g_\phi(\Delta\Theta_\ell), \quad \Theta_s^* \leftarrow \text{Inject}(\Theta_s, \widehat{\Delta\Theta}_s).$$

Using a static neuron-level attribution method, LaTen scores neurons in both FFN and MHSA (per selected layer; last-useful-token based) and selects the top- k neurons per layer for transfer, motivated by evidence that neurons serve as units storing skills/knowledge; this yields vectorized teacher deltas $\Delta\Theta_\ell$ over chosen FFN/MHSA submodules.

To bridge width/depth gaps and value-scale discrepancies, a small two-layer MLP *hypernetwork* g_ϕ (with ReLU) is trained on a tiny *alignment* set (often < 100 examples) to map teacher deltas into student-shaped deltas by minimizing the LM loss while the base weights remain frozen:

$$\min_{\phi} \mathbb{E}_{(x,y) \in \mathcal{D}_{\text{align}}} \mathcal{L}_{\text{LM}}(y; M_s(x; \Theta_s \oplus g_\phi(\Delta\Theta_\ell))).$$

After learning g_ϕ , $\widehat{\Delta\Theta}_s$ is injected once, aiming for immediate gains without further training. LaTen contrasts this with SEEKING's SVD-to-LoRA initialization, and attributes transfer instability to *neural incompatibility* (low similarity across behavioral and parametric spaces) when deltas are unaligned. Experiments show promising (though not uniformly stable) improvements under PrePKT and comparisons against baselines such as self-derived LoRA and language-based distillation.

C DISCUSSION

C.1 MEDIUM IN PARAMETRIC KNOWLEDGE TRANSFER.

Compare with the prior work such as Seeking and LaTen, which take model weights as the medium for knowledge transfer, SEMALIGN suggest using layer outputs as the medium. Our approach shows

702 advantages in efficacy, and also, requires almost no computation cost for alignment. Moreover, our
 703 methodology have theoretically better performance based on the following reasons.
 704

705 For the perspective of information transfer, layer outputs as the medium requires less bandwidth than
 706 the prior work of PKT, as well as the general knowledge transfer work. Because in language models,
 707 the dimension size of layer outputs is much smaller than that of layer parameters, as well as that of
 708 the probabilities in LM vocabulary. A smaller size indicates less information to transfer. Therefore,
 709 transferring more knowledge of same quality requires more computation cost; or, transferring more
 710 knowledge by costing same computation indicates high information loss.

711 From the perspective of the association between knowledge and neurons, layer outputs is a better
 712 choice than layer parameters. It is known by prior work that LM knowledge and neurons follow
 713 many-to-many dynamic associations (Allen-Zhu & Li). Therefore, if knowledge transfer is con-
 714 ducted through layer parameters (especially LaTen), certain student’s parameters will be updated
 715 with certain teacher’s parameters. However, no matter the layer parameters from the teacher or
 716 student model, they associate with not only the current given data, but also other data. Such prac-
 717 tice of parametric knowledge transfer by direct parameter manipulation is likely to cause potential
 718 side effects. In contrast, Seeking indicates a safer practice, which introduces the idea of parametric
 719 knowledge transfer to the framework of parameter-efficient finetuning.

720 C.2 LIMITATIONS AND FUTURE WORK

721 Our study focuses on a limited set of tasks, and layer-level pairing, while broader coverage (archi-
 722 tectures, modalities, safety-critical settings) remains open. Future directions include: (1) extending
 723 semantic alignment to finer granularity (sub-layer, attention head) (2) comparing objectives that
 724 combine causal and semantic constraints; (3) exploring better strategies on layer pairing based on
 725 the layer outputs in teacher and student models; (4) scaling analyses across families with larger
 726 architectural gaps to stress-test robustness. We hope SemAlign serves as a simple, practical foun-
 727 dation for activation-driven knowledge transfer and as a stepping stone toward precise, low-loss
 728 “brainwave” communication between models.

729
 730
 731
 732
 733
 734
 735
 736
 737
 738
 739
 740
 741
 742
 743
 744
 745
 746
 747
 748
 749
 750
 751
 752
 753
 754
 755